Optica Applicata, Vol. XXVII, No. 2, 1997

Analysis of the optical properties of thin films using the transmission line method

A. J. ABU EL-HAIJA*

Physics Department, Al Al-Bayt University, Mafraq, Jordan.

A method of applying the transmission line matrix (TLM) technique to calculate the optical properties of dielectric and conducting thin films is described. The method offers a powerful alternative to the characteristic matrix technique. The obtained values of the reflectivity R, and transmissivity T, for standard cases compared remarkably with their values that are well established by other techniques. The advantages of the present method reside in the successful replacement of the film (dielectric or absorbing) by transmission line segments in a model that exemplifies the thin film effectively without the need of working with matrices whose elements are generally complex. This TLM technique enables a much easier treatment of the optical properties of ideal periodic structures, perturbed multilayer structures and superlattices.

1. Introduction

The calculation of the optical properties of thin films and multilayer structures has advanced tremendously in the last two decades. The intense attention which this problem acquired has stemmed from the high state of perfection attained in the fabrication of thin films, multilayer structures and superlattices and in the profound progress achieved in the measurement and calculation of their optical properties, as well. The thoeretical computation of these properties, however, has demonstrated increasing interest in applying the characteristic matrix technique which will be abbreviated here as CMT. The CMT method has proved to be efficient and very general, particularly after the development of a successful computer program for handling conducting thin films and multilayer systems that consist of arbitrary dielectric conducting individual layers utilizing the CMT [1], [2]. Adequate acquaintance with the CMT technique can be achieved by referring to the above references and those originally reported at the early initiation and progress of this method [3]–[5]. The present paper exposes a new method known as the Transmission Line Matrix (TLM) method for utilization in problems of thin films and multilayer systems. Therefore, the context of this article will be mainly devoted to the TLM basic theory revealing the features that made its adoption to thin films possible. In this work, the potential and capacity of the TLM in treating inhomo-

* On leave from the University of Jordan.

geneous waveguide problem are utilized. The method evolved in the seventies [6], [7] and has been effectively extended in few years to offer numerical solutions for electromagnetic wave propagation [8], diffusion problems [9], [10], and first order rate equations [11]. The technique uses open circuited stubs of variable characteristic impedance at each node in the matrix, thereby providing an analog for a dielectric. This makes it possible to calculate 2-dimensional scattering problems using the TLM. Accordingly, the adoption of the TLM, which is a time domain technique, to calculate the optical properties of a semi-infinite homogeneous dielectric material is at the present of no basic difficulty. However, the adoption of this method to calculate the optical properties of thin films (dielectric and absorbing), as presented here, is the purpose of the present article with the intention to boost the capacity of the method so that one can calculate and analyze the optical properties of periodic layer systems and arbitrary multilayer structures, an aspect which to the best of the author's knowledge has not been handled fully yet. As a matter of fact, the method provides a rather practical efficient way of computing the optical properties of ideal and non-ideal superlattices using the TLM on a personal computer. This would offer further enhancement of the problem of superlattices previously handled by the author [1], [2], [12]. Moreover, the waveform in the three regions – I, II and III, representing media of incidence, film and ambient, respectively, has been calculated and plotted. The changes in the wave number in regions II and III correspond very well with the analytic solution of the problem.

The present paper as it stands here serves two purposes. It introduces the method with all its basic theory, derivations and nomenclature and validates its legitimacy through presenting a few examples as calculated via this TLM method; these are sketched and analyzed in Sec. 4. An algorithm appropriate for such cases is developed and full analogy between corresponding terms in electromagnetic theory and TLM is made in the next section.

2. Theory

2.1. Dielectric interface

Consider a plane electromagnetic wave propagating in the X direction and incident on an interface extending in the Y-Z plane, as shown in Fig. 1. Maxwell's curl equations for the electric field E_y and magnetic field H_z give:

$$\frac{\partial H_z}{\partial x} = -\varepsilon_1 \frac{\partial E_y}{\partial t} \tag{1}$$

and

$$\frac{\partial E_y}{\partial x} = -\mu_1 \frac{\partial H_z}{\partial t} \tag{2}$$

where ε_1 and μ_1 are the medium permittivity and permeability, respectively.

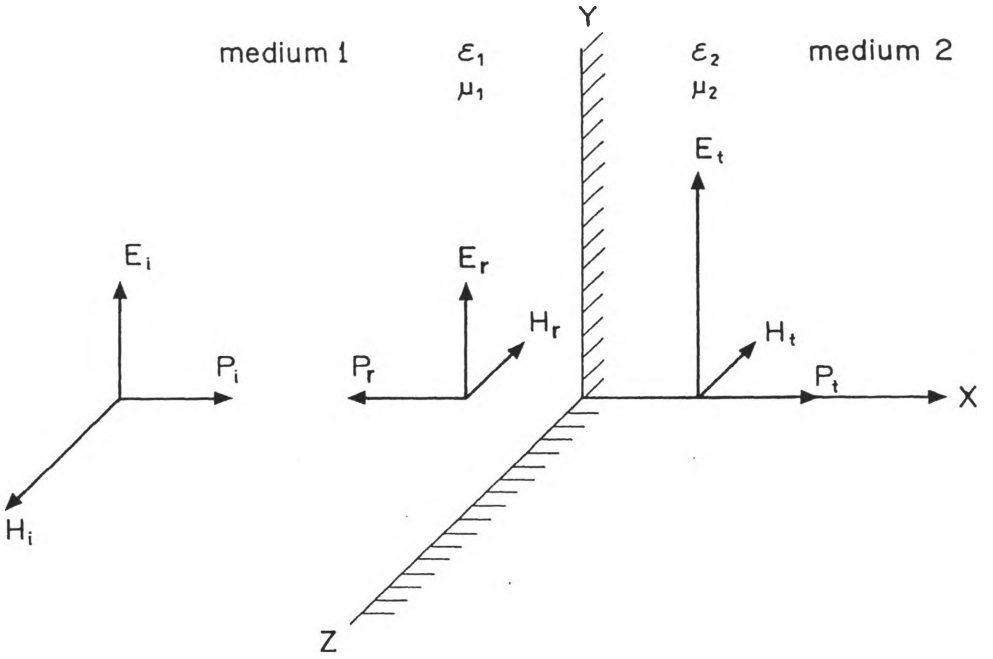

Fig. 1. Schematic representation of the incident, reflected and transmitted electric and magnetic field amplitudes at the interface between two media. Those amplitudes are denoted by the subscripts *i*, *r* and *t*, respectively

Combining the above two equations yields the wave equation

$$\frac{\partial^2 E_y}{\partial x^2} = \frac{1}{U_1^2}\frac{\partial^2 E_y}{\partial t^2}, \tag{3}$$

with $U_1 = 1/\sqrt{\varepsilon_1 \mu_1}$ being the wave velocity in medium 1. If $\mu_1 = 1$, then the refractive index

$$n = \frac{U_0}{U_1} = \sqrt{\varepsilon_{r1}}$$

where U_0 denotes the wave velocity in free space and ε_{r1} is the relative permeability of the medium of incidence, medium 1. The general solution to the above wave equation in medium 1 takes the form

$$E_1 = E_i(e^{j\omega(t-n_1 x/U_0)} + \rho_{12} e^{j\omega(t+n_1 x/U_0)} \tag{4}$$

where the first term represents the incident wave on the interface and the second term represents the reflected wave from the interface. The reflection coefficient ρ_{12}, obtained from the continuity of the field components tangential to the interface, is given by

$$\rho_{12} = \frac{E_i}{E_r} = \frac{(n_1 - n_2)}{(n_1 + n_2)}. \tag{5}$$

Defining the wave impedance Z_m in medium m by

$$Z_m = \frac{E_i}{H_i} = \frac{E_r}{H_r} = \sqrt{\mu_m/\varepsilon_m}, \tag{6}$$

it can be shown that

$$\rho_{12} = \frac{(Z_2 - Z_1)}{(Z_2 + Z_1)}. \tag{7}$$

The electric field in the second medium is given by

$$E_2 = E_t e^{j(\omega t - n_2 x/U_0)} = (1 + \rho_{12}) E_i e^{j(\omega t - n_2 x/U_0)}. \tag{8}$$

The transmission coefficient τ_{12}, defined as $\tau_{12} = E_t/E_i$, can be expressed in the form

$$\tau_{12} = \frac{2Z_2}{(Z_2 + Z_1)} = \frac{2n_1}{(n_1 + n_2)} = 1 + \rho_{12}. \tag{9}$$

The reflectivity R and transmissivity T, representing the average power reflected from and transmitted across the interface, are given by:

$$R = \frac{E_r^2/Z_1}{E_i^2/Z_1} = \rho_{12}^2,$$
$$T = \frac{E_t^2/Z_2}{E_i^2/Z_1} = \frac{n_2}{n_1}\tau_{12}^2, \tag{10}$$

and these are related to each other through the principle of energy conservation or

$$R + T = 1. \tag{11}$$

2.2. Thin film

The analysis of the reflection and the transmission of a plane wave by a thin dielectric or absorbing film is well established and is almost a textbook material [13]. Therefore, efforts will be made to avoid all unnecessary details and derivations. However, establishing the TLM as a new tool for computing the optical properties of thin films seems impossible without laying down the essential elements of the procedure and comparing them with their counterparts in electromagnetic theory and the characteristic matrix method. This bit of discomfort is unavoidable if a smooth transfer to the new method is required. On the computational level, the characteristic matrix technique represents a thin film by a matrix which contains all parameters pertinent to the film, such as thickness, refractive index, which is generally complex, and the incident wavelength. The method enables calculation of the reflection and transmission coefficients at the boundaries of the film (Fig. 2). In notations frequently used by scientists with an engineering background, an equi-

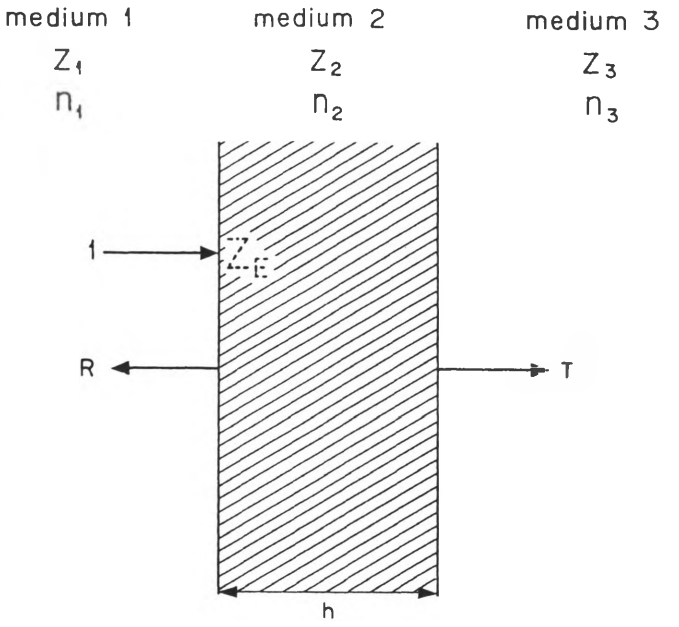

Fig. 2. Schematic representation of a thin dielectric film of thickness h and refractive index n_2. The intensity of the incident e.m. wave is taken as unity

valent approach is made through introducing the term known as the equivalent wave impedance Z_E encountered by the plane wave at the boundary, and this is given by

$$Z_E = Z_2 \frac{Z_3 + jZ_2 \tan(\beta_2 h)}{Z_2 + jZ_3 \tan(\beta_2 h)} \tag{12}$$

where h represents the film thickness and β_2 is the wave number in the film defined as

$$\beta_2 = \frac{2\pi}{\lambda} = \frac{\omega}{U_2}. \tag{13}$$

The reflection coefficient of the film which has a complex value indicating an amplitude and phase changes is given by

$$\rho_{12} = \frac{Z_E - Z_1}{Z_E + Z_1}. \tag{14}$$

The reflectivity R and the transmissivity T are then obtained from

$$R = \frac{Z_E - Z_1}{Z_E + Z_1},$$

$$T = 1 - R. \tag{15}$$

2.3. Absorbing medium

For an absorbing medium, however, a plane wave propagating in the X direction with its dielectric field polarized in the Y direction, the electric field E_y gets attenuated along the X direction due to the conductivity of the medium σ which appears in Maxwell's curl equations as follows:

$$\frac{\partial H_z}{\partial x} = -\varepsilon \frac{\partial E_y}{\partial t} - \sigma E_y, \tag{16}$$

$$\frac{\partial E_y}{\partial x} = -\mu \frac{\partial H_z}{\partial t}. \tag{17}$$

Combining the above equations gives

$$\frac{\partial^2 E_y}{\partial x^2} = \varepsilon\mu \frac{\partial^2 E_y}{\partial t^2} + \sigma\mu \frac{\partial E_y}{\partial t}. \tag{18}$$

For sinusoidal time varying fields, E_y and H_z relate to each other through the following:

$$\frac{\partial H_z}{\partial x} = -(j\omega\varepsilon + \sigma)E_y,$$

$$\frac{\partial E_y}{\partial x} = -\mu H_z, \tag{19}$$

which may also be combined giving

$$\frac{\partial^2 E_y}{\partial x^2} = j\omega\mu(\sigma + j\omega\varepsilon)E_y = \gamma^2 E_y \tag{20}$$

where

$$\gamma = \sqrt{j\omega\mu(\sigma + j\omega\varepsilon)} = j\omega\sqrt{\mu\varepsilon}(1 - j\sigma/\omega\varepsilon)^{1/2}. \tag{21}$$

For a good dielectric $\sigma/\omega\varepsilon < 0.1$ and the r.h.s. of Eq. (21), the latter can be expanded as follows:

$$\gamma = j\omega\sqrt{\mu\varepsilon}\left(1 - \frac{j\sigma}{2\omega\varepsilon} + \frac{\sigma^2}{8\omega^2\varepsilon^2} + \ldots\right) = j\omega\sqrt{\mu\varepsilon}\left(1 - \frac{j\xi}{2} + \frac{\xi^2}{8} + \ldots\right)$$

where

$$\xi = \frac{\sigma}{\omega\varepsilon}. \tag{22}$$

Keeping only the first two terms, γ becomes

$$\gamma = j\omega\sqrt{\mu\varepsilon}\left(1 - \frac{j\xi}{2}\right). \tag{23}$$

Thus writing γ in the general complex form

$$\gamma = \alpha + j\beta, \tag{24}$$

with

$$\alpha = \omega\sqrt{\mu\varepsilon}\frac{\xi}{2}, \quad \beta = \omega\sqrt{\mu\varepsilon}. \tag{25}$$

The solution to Equation (20) can be written in the form

$$E_y = E_i e^{-\alpha x} e^{j(\omega t - \beta x)}, \tag{26}$$

giving

$$H_z = \frac{E_i}{Z_0^*} e^{-\alpha x} e^{j(\omega t - \beta x)} \tag{27}$$

where Z_0^* represents the complex wave impedance which is now given by

$$Z_0^* = \sqrt{\mu/\varepsilon}\left(1 + \frac{j\xi}{2}\right). \tag{28}$$

The solution to Equation (24) can equally be expressed in terms of a complex index of refraction

$$n^* = n_{re} - jn_{im}. \tag{29}$$

That is,

$$E_y = E_i e^{j\omega(t - n^* x/U_0)} = E_i e^{-\omega n_{im} x/U_0} e^{j(\omega t - \omega n_{re} x/U_0)}. \tag{30}$$

Comparing Equations (26) and (30) results in the following equivalence:

$$\alpha = \frac{\omega n_{im}}{U_0} = \omega\sqrt{\mu\varepsilon}\frac{\xi}{2},$$

$$\beta = \frac{\omega n_{re}}{U_0} = \omega\sqrt{\mu\varepsilon}. \tag{31}$$

Algebraic manipulation of Equations (31) gives for non-magnetic materials ($\mu_r = 1$):

$$n_{re} = \sqrt{\varepsilon_r}, \tag{32a}$$

$$n_{im} = \sqrt{\varepsilon_r}\xi/2, \tag{32b}$$

$$n^* = \sqrt{\varepsilon_r}(1 - j\xi/2). \tag{32c}$$

3. The TLM method

3.1. Basic Transmission Line Theory

In their efforts to introduce a numerical solution for two dimensional scattering problems, Johns and Beurle initiated the representation of Maxwell's equations by the transmission line matrix method. The basic idea in the model comes from the

transmission line consisting of two parallel conductors separated by a dielectric material. The conductors may be parallel wires or coaxial cylinders. This physical arrangement leads to an inductance L_d and capacitance C_d between the conductors distributed over the length of the line. A transmission line segment of length Δx can be represented by the equivalent lumped circuit of Fig. 3. Basic transmission line

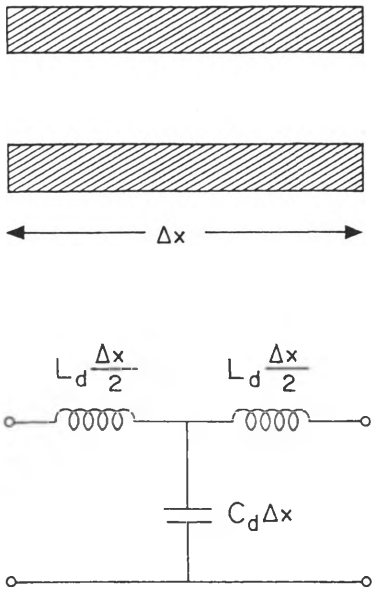

Fig. 3. Transmission line segment of length Δx and an equivalent lumped circuit

theory shows that the voltage and current variations along the line may be described by a wave equation. The speed of the wave is related to the inductance and capacitance per unit length L_d and C_d, respectively, through the relation

$$U_0 = 1/\sqrt{L_d C_d}. \tag{33}$$

The voltage wave may reflect at the end of the line if the load impedance Z_L is not matched with the transmission line characteristic impedance Z_0 which is equal to $\sqrt{L_d/C_d}$. Denoting the reflection coefficient by ρ at the load, it can be shown that

$$\rho = (Z_L - Z_0)/(Z_L + Z_0) = (Y_0 - Y_L)/(Y_0 + Y_L) \tag{34}$$

where $Y_0 = 1/Z_0$ and $Y_L = 1/Z_L$ represent the admittance of the line and the load, respectively. The relationship between the incident, reflected and transmitted voltages and currents at the load is summarized in Fig. 4. The equivalent impedance Z_E of a transmission line segment of length Δx and characteristic impedance Z_0 connected to a load Z_L is given by

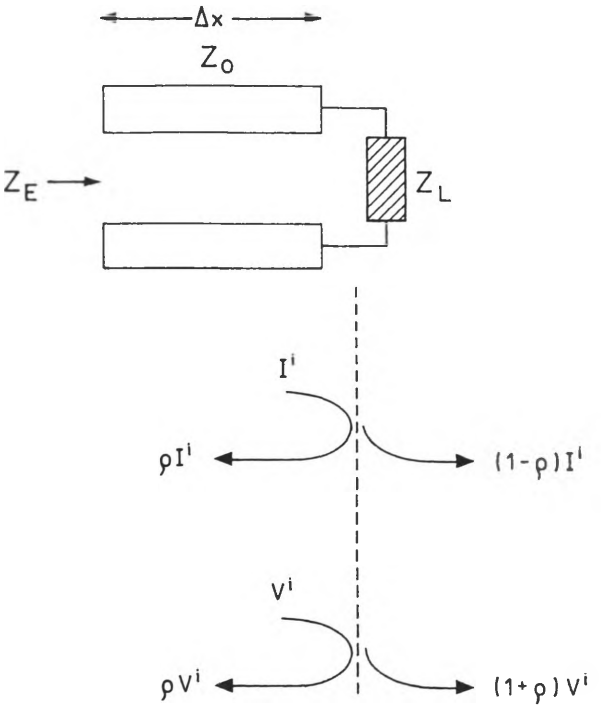

Fig. 4. Reflection and transmission of voltage and current pulses at mismatched load impedance Z_L

$$Z_E = Z_0 \frac{Z_L + jZ_0 \tan(\beta \Delta x)}{Z_0 + jZ_L \tan(\beta \Delta x)} \tag{35}$$

where $\beta = \omega/U_0 = 2\pi/\lambda$. Transmission line theory also shows that an open circuited transmission line ($Z_L \to \infty$) of finite length (a stub) has a capacitive impedance ($Z_E = 1/j\omega C$) that depends on the length and characteristic impedance of the stub (Z_s). When $Z_L \to \infty$, the equivalent impedance Z_E of the open circuited stub takes the form

$$Z_E = 1/j\omega C = Z_s/j \tan(\beta \Delta x). \tag{36}$$

For small angles $\tan(\beta \Delta x) \simeq \beta \Delta x = \omega \Delta x/U$ and the stub capacitance C becomes

$$C = \Delta t/Z_s = \Delta t Y_s \tag{37}$$

where Y_s is the stub characteristic admittance and Δ is the time taken by a voltage wave to travel along the stub length. The voltage wave reflects at the open circuited end of the stub with $\rho = +1$.

3.2. Discrete model of a loss free space

3.2.1. The TLM structure

The propagation space may be quantized into equally spaced scattering zones (nodes). Each node is modelled by a junction of an ideal transmission line segment of

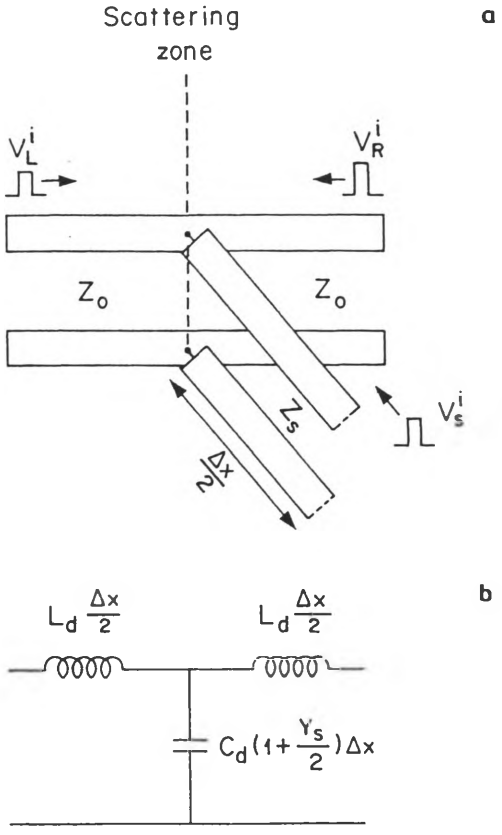

Fig. 5. TLM mode that represents a length Δx of a loss free medium (a), and an equivalent lumped circuit (b)

length Δx and characteristic impedance Z_0 and an open circuit stub of length $\Delta x/2$ and characteristic impedance Z_s. The stub is connected to the midpoint of the transmission line segment as shown in Fig. 5a. If the voltage pulse travels along the line and the stub at the same speed, then

$$\frac{\Delta x}{\Delta t} = \frac{1}{\sqrt{L_d C_d}}, \quad Z_0 = \sqrt{L_d/C_d}, \text{ and}$$
$$\frac{\Delta x}{\Delta t} Z_0 = \frac{1}{C_d}. \tag{38}$$

The lumped capacitance at the node due to the transmission line only is

$$C_d \Delta x = \frac{\Delta t}{Z_0}. \tag{39}$$

Similarly, the lumped capacitance at the node due to the stub is

$$C_s \frac{\Delta x}{2} = \frac{\Delta t/2}{Z_s} \tag{40}$$

where C_s represents the distributed capacitance of the stub. If the transmission line admittance $Y_0 = 1/Z_0$ is taken as unity and the stub admittance Y_s is normalized to that of the line, then $C_s/C_d = Y_s$ and the total lumped capacitance at the node becomes

$$C_s\frac{\Delta x}{2} + C_d\Delta x = C_d(Y_s/2+1)\Delta x. \tag{41}$$

The equivalent lumped circuit of the transmission line and the stub is shown in Fig. 5b. Analysis of the equivalent circuit gives the following relationship between the voltage and current in the line:

$$\frac{\partial V}{\partial x} = -L_d\frac{\partial I}{\partial t}, \tag{42}$$

$$\frac{\partial I}{\partial x} = -C_d(1+Y_s/2)\frac{\partial V}{\partial t}. \tag{43}$$

Combining the above equation gives

$$\frac{\partial^2 V}{\partial x^2} = \frac{1}{U^2}\frac{\partial^2 V}{\partial t^2} \tag{44}$$

where $U = 1/\sqrt{L_dC_d(1+Y_s/2)}$ and represents the velocity of the voltage wave in the periodic structure of transmission lines and stubs. The wave velocity in a transmission line segment is $U_0 = 1/\sqrt{L_dC_d}$. Therefore, the additional capacitance at the node due to the stub results in a slower wave in the structure with $U = U_0/\sqrt{1+Y_s/2}$. A comparison between Eqs. (42)–(44) and (1)–(3) yields the following equivalence between the voltages and currents in the line and the electric and magnetic fields of Maxwell's equations:

$$\begin{aligned} &V \equiv E_y,\\ &I \equiv H_z,\\ &C_d \equiv \varepsilon_0,\\ &L_d \equiv \mu_0,\\ &(1+Y_s/2) \equiv \varepsilon_r. \end{aligned} \tag{45}$$

Thus the voltage in the matrix models the electric field in the medium and the stub admittance models a loss free medium with a refractive index n such that

$$Y_s = 2(n^2-1). \tag{46}$$

3.2.2. Scattering algorithm

Time is also quantized in TLM. The electric field E_y is represented by a train of discrete voltage impulses at Δt-seconds' interval. The amplitude of the voltage impulses corresponds to the electric field value at the corresponding time interval. The numerical solution to the TLM model is based on the scattering of voltage impulses at the node due to mismatch of impedances. Let ${}_kV_L^i$ represent the

voltage pulse incident at node N from the left branch at the k-th time interval as shown in Fig. 5a. The load impedance encountered by ${}_kV_L^i$ is the parallel combination of Z_s and Z_0 or the load admittance $Y_L = 1 + Y_s$. Therefore, the reflection coefficient from the left-hand side of the node ρ_L is given by

$$\rho_L = \frac{1 - Y_L}{1 + Y_L} = \frac{-Y_s}{2 + Y_s}. \tag{47}$$

The reflected voltage pulse $\rho_L {}_kV_L^i$ travels Δx meters through the left branch to become incident on the right-hand side of node $(N-1)$. Similarly, the transmitted voltage pulse $(1+\rho_L){}_kV_L^i = \frac{2}{2+Y_s} {}_kV_L^i$ travels along the right branch to become incident on node $(N+1)$ after Δt seconds. The voltage pulse transmitted to the stub, which has the value $\frac{2}{2+Y_s} {}_kV_L^i$, travels to the open circuited end in $\Delta t/2$ seconds where it reflects back to become incident on the same node after another $\Delta t/2$ seconds. A similar analysis applies to the voltage pulses incident from the right ${}_kV_L^i$ and the stub ${}_kV_s^i$ due to the scattering at the previous time interval. The principle of superposition combines the effect of the voltage pulses incident from the three branches to give

$$\begin{vmatrix} {}_kV_R^r \\ {}_kV_L^r \\ {}_kV_s^r \end{vmatrix} = \frac{1}{2+Y_s} \begin{vmatrix} -Y_s & 2 & 2Y_s \\ 2 & -Y_s & 2Y_s \\ 2 & 2 & Y_s - 2 \end{vmatrix} \begin{vmatrix} {}_kV_R^i \\ {}_kV_L^i \\ {}_kV_s^i \end{vmatrix}. \tag{48}$$

An alternative representation to the above matrix may be given in terms of the node voltage A, where

$$A = \frac{2}{2+Y_s} ({}_kV_R^i + {}_kV_L^i + Y_s \, {}_kV_s^i), \tag{49}$$

and

$$\begin{aligned} {}_kV_R^r &= A - {}_kV_R^i, \\ {}_kV_L^r &= A - {}_kV_L^i, \\ {}_kV_s^r &= A - {}_kV_s^i; \end{aligned} \tag{50}$$

the values ${}_kV_R^r$, ${}_kV_L^r$ and ${}_kV_s^r$ represent the scattered voltage pulses into the corresponding branches. The voltage pulses incident on the node at iteration interval $k+1$ are those scattered from neighbouring ones and the stub at iteration interval k, or:

$$\begin{aligned} {}_{k+1}V_R^i(N) &= {}_kV_L^r(N+1), \\ {}_{k+1}V_L^i(N) &= {}_kV_R^r(N-1), \\ {}_{k+1}V_s^i(N) &= {}_kV_s^r(N). \end{aligned} \tag{51}$$

Equations (50) and (51) are generally called the scattering and connection algorithms, respectively.

3.2.3. Outer boundary conditions

The TLM may only represent a limited length in space. Therefore, the outer transmission line segments are terminated by Z_L and Z_R which represent the characteristic wave impedances of the media that lie on the left- and right-hand sides of the mesh, respectively. The mesh is excited with a voltage source E_s through the impedance Z_L as shown in Fig. 6; E_s represents a sinusoidal source of electric field and is given by

$$E_s = E_{\max}\sin(2\pi U t/\lambda). \tag{52}$$

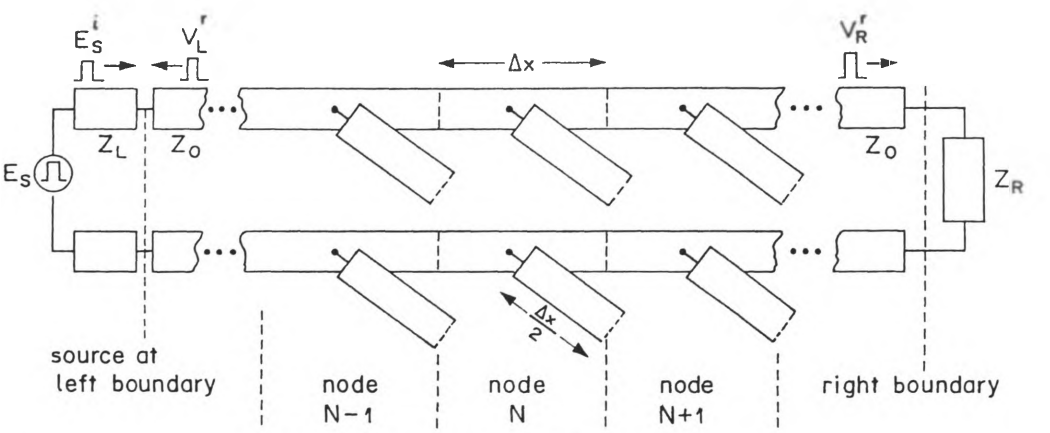

Fig. 6. Transmission line model of the propagation space

In discrete time and space $t = k\Delta t$ and $U = \Delta x/\Delta t$, therefore

$${}_kE_s = E_{\max}\sin(2\pi k\Delta x/\lambda). \tag{53}$$

The voltage pulse launched by the source at iteration interval k combines with the pulse reflected to the left from the first node ${}_kV_L^r$ to give the new incident pulse on the first node from the left at the next iteration interval. The voltage pulse ${}_{k+1}V_L^r$ may be obtained by pulse analysis using the superposition principle and the reflection coefficient encountered by each incident pulse to give

$${}_{k+1}V_L^i = \frac{Z_L - Z_0}{Z_L + Z_0}\,{}_kV_L^r + \frac{2Z_0}{Z_L + Z_0}\,{}_kE_s^i. \tag{54}$$

If the medium on the left-hand side is free space, then $Z_L = Z_0$ and

$${}_{k+1}V_L^i = {}_kE_s^i. \tag{55}$$

Similar treatment on the right boundary gives the voltage incident from the left branch of the last node as

$$_{k+1}V_R^i = \frac{Z_R - Z_0}{Z_R + Z_0}\,{}_kV_R^r + \frac{1-n_R}{1+n_R}\,{}_kV_R^r \tag{56}$$

where n_R is the refractive index of the medium on the right-hand side of the mesh.

3.3. TLM model of an absorbing medium

The complex refractive index n^*, which represents losses in the medium due to the conductivity term in Maxwell's equations, may be represented in TLM by adding a shunt resistor R at the node, as shown in Fig. 7. The stub admittance Y_s and

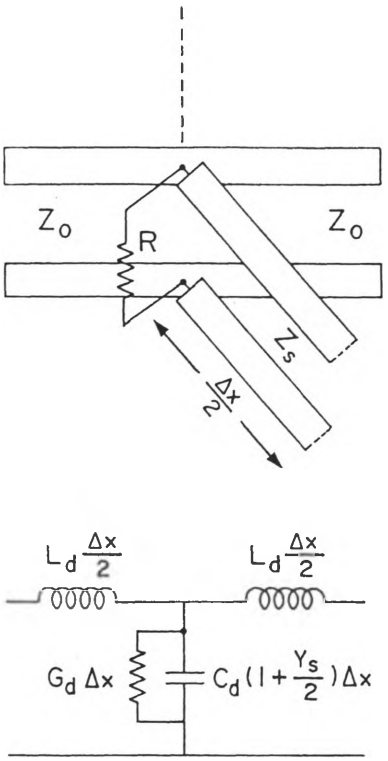

Fig. 7. TLM node that stands for a length Δx of a lossy medium and the equivalent lumped circuit

the resistor conductance $G = 1/R$ are normalized to the basic transmission line characteristic admittance Y_0 which is taken as unity. Voltage and current analysis of the equivalent circuit gives

$$\frac{\partial I}{\partial x} = -C_d(1+Y_s/2)\frac{\partial V}{\partial t} - g_d V, \tag{57}$$

$$\frac{\partial V}{\partial x} = -L_d\frac{\partial I}{\partial t}, \tag{58}$$

where $g_d = G/\Delta x$ represents the distributed conductance at the node. Combining the above equations gives

$$\frac{\partial^2 V}{\partial x^2} = L_d C_d (1 + Y_s/2) \frac{\partial^2 V}{\partial t^2} + L_d g_d \frac{\partial V}{\partial t}. \tag{59}$$

Comparing Equations (57)–(59) with Equations (16)–(18) yields the following equivalence

$$\begin{aligned} &V \equiv E_y, \quad I \equiv H_z, \\ &C_d \equiv \varepsilon_0, \quad L_d \equiv \mu_0, \\ &(1 + Y_2/2) \equiv \varepsilon_r, \quad g_d \equiv \sigma. \end{aligned} \tag{60}$$

Thus the voltage wave in the TLM structure represents the electric field in the lossy medium. For correct modeling of the absorbing medium, the real and imaginary parts of the refractive index n^* must be mapped into the appropriate values of G and Y_s in the TLM structure. Using Eq. (32), ε_r and σ may be expressed in terms of n_{re} and n_{im} as:

$$\sigma = 2\omega\varepsilon_0 n_{re} n_{im}, \tag{61a}$$

$$\varepsilon_r = n_{re}^2. \tag{61b}$$

Replacing σ by g_d and ε_0 by C_d in Eqs. (61) yields:

$$g_d = 2\omega C_d n_{re} n_{im}, \tag{62}$$

or

$$\frac{G}{\Delta x} = \frac{4\pi \Delta x}{\lambda \Delta t} C_d n_{re} n_{im}. \tag{63}$$

Equations (38) give $\frac{\Delta x}{\Delta t} C_d = 1$ for a unit line admittance. Therefore,

$$G = 4\pi \frac{\Delta x}{\lambda} C_d n_{re} n_{im}. \tag{64}$$

Also, upon replacing ε_r by $(1 + Y_s/2)$ in Eq. (61b) we obtain

$$Y_s = 2(n_{re}^2 - 1). \tag{65}$$

Equations (64) and (65) map the complex refractive index into a stub admittance Y_s and resistor conductance G at an arbitrary node in the TLM space. The scattering algorithm described by Eqs. (49)–(51) is now modified to take account of the shunt resistor and takes the general form

$$A = \frac{2}{2 + Y_s + G} ({}_k V_R^i + {}_k V_L^i + Y_{s\,k} V_s^i), \tag{66}$$

and

$$
\begin{aligned}
{}_kV_R^r &= A - {}_kV_R^i, \\
{}_kV_L^r &= A - {}_kV_L^i, \\
{}_kV_s^r &= A - {}_kV_s^i.
\end{aligned} \tag{67}
$$

4. Results and discussion

The presentation of results starts with the illustration of the propagation of electromagnetic radiation in a thin dielectric film (Fig. 8). For this purpose a one-dimensional TLM model of length 240 Δl is set up in the computer. The model is

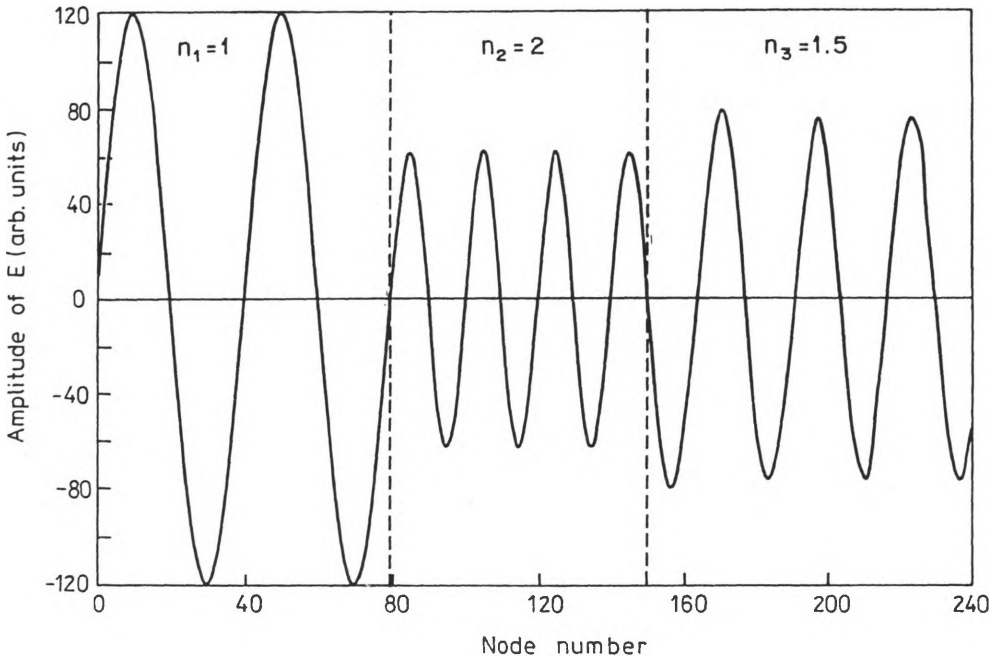

Fig. 8. Illustration of the amplitude of the electric field of an electromagnetic wave in the media of incidence, a dielectric film of $n = 2.0$ and medium of transmittance (last medium). The media are 1, 2 and 3, respectively

divided into three regions of lengths $80\Delta l$, $70\Delta l$ and $90\Delta l$ which represent free space, a dielectric film and a substrate, respectively. Their refractive indices n_1, n_2 and n_3 are assigned the values 1, 2 and 1.5, respectively. The value of the substrate index of refraction being 1.5 corresponds to quartz near $\lambda \approx 5000$ Å which is widely used in the deposition of thin films. Therefore, from Eq. (65) the stub admittance Y_s for all nodes in the corresponding regions are 0, 6 and 2.5, respectively. The substrate is assumed to stretch from the right boundary of the model to ∞. Accordingly, the reflection coefficient of the right boundary $\rho_R = \dfrac{1-n_3}{1+n_3} = -0.2$. The TLM structure

is excited from the left branch of the first node where free space is assumed to stretch from $-\infty$ to the first node. The excitation is represented by a voltage source with peak value of 100 V and wavelength $\lambda = 40\Delta l$. The model is solved for 500 iterations that correspond to 12.5 cycles. The plot sketched in Fig. 8 displays the node voltage versus position after 500 iterations and manifests the continuity of the electric field (node voltage) at the two surfaces of the dielectric. It also shows that $\frac{\lambda_2}{n_2} = \frac{\lambda_3}{n_3} = \lambda$.

As a next step the reflectivity of a dielectric thin film is calculated. Here a stub loaded one dimensional TLM model of 200 nodes is used to represent such a film of refractive index n_2 and thickness h. The film is mounted on a substrate of refractive index $n_3 = 1.5$. A source of electromagnetic radiation of wavelength $\lambda = 80\Delta l$ in free space ($n_1 = 1$) is represented by a sinusoidal voltage source which excites the TLM structure through the first node as given by Eq. (55). The reflectivity of the film is measured for various values of n_2 and h. The film is assigned a value for n_2 by choosing the corresponding value for the stub admittance Y_s for all nodes that represent the film according to Eq. (46). Initially, the film is located between nodes 101 and 110 ($h = 10\Delta l$). The thickness of the film is increased in steps of Δl and the mesh is solved for 500 iterations for each set of values of n_2 and h. The voltage waveform at any point in region I which corresponds to free space is the sum of the electric field components due to the wave incident on the film and that reflected from the film. If the sinusoidal signal $A_{81}(k)$ denotes the voltage waveform (electric field) at node 81, then the incident electric field component is in phase and equals the source signal. This is so since the distance between them is one full wavelength. The waveform $f(k)$ which corresponds to the reflected field component is given by

$$f(k) = A_{81}(k) - E_{\max} \sin\left(\frac{2\pi k \Delta l}{\lambda}\right). \tag{68}$$

By taking $f_{\max}$ to represent the peak value of the sinusoidal signal $f(k)$ for the last 100 iterations, the reflectivity and, accordingly, the transmissivity of the film are obtained from the relationship

$$R = \left(\frac{f_{\max}}{E_{\max}}\right)^2, \quad T = 1 - R. \tag{69}$$

Figure 9 shows the reflectivity patterns obtained using the TLM method for $n_2 = 1.5$, 1.7, 2 and 2.5. The theoretical curves are obtained from Eqs. (12)–(15). These curves were found identical to curves computed for films of identical indices of refraction using the transfer matrix technique. For the sake of comparison and clarity, calculations executed by both methods are displayed on each curve.

The last example handled by the method in this article is the calculation of the reflectivity and transmissivity of an absorbing film. To accomplish this for a thin absorbing film, the TLM setup of 200 nodes described earlier is used to measure the reflectivity and transmissivity of the film. The complex refractive index n_2^* of the film is modelled by a stub admittance Y_s and resistor conductance G for all nodes that

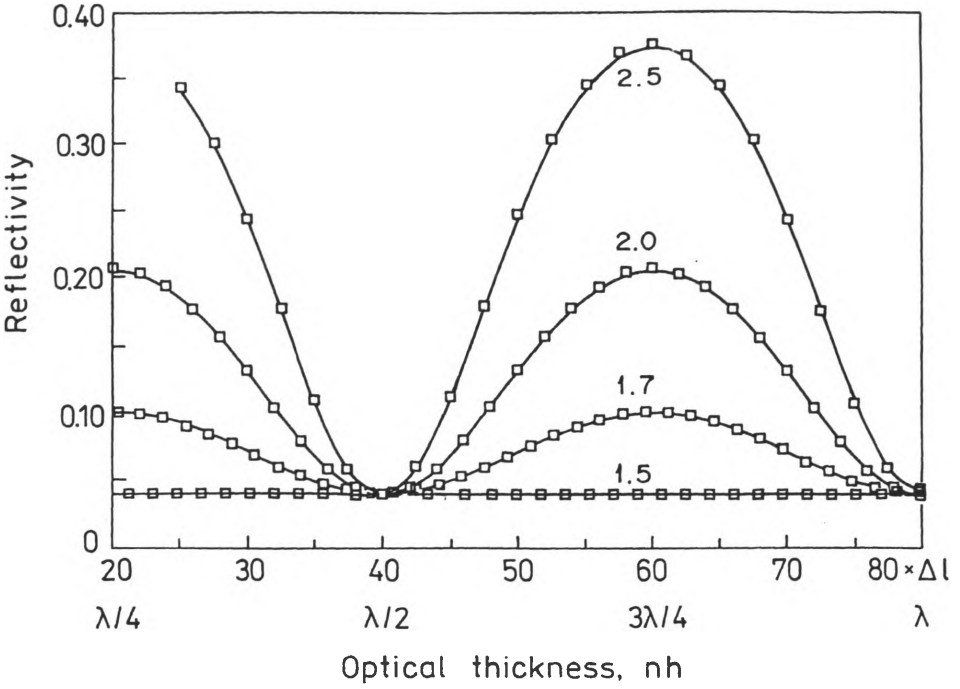

Fig. 9. Calculation of the reflectivity R versus the optical thickness of thin dielectric films of refractive indices 1.5, 1.7, 2.0 and 2.5. □ — values obtained by the TLM method, and —— values obtained by the CMT technique

represent the film according to Eqs. (72) and (73). The film is initially located between nodes 101 and 110 ($h = 10\Delta l$). The thickness of the film is increased in steps of Δl and the mesh is solved for 500 iterations for each set of the values of h, n_{re} and n_{im}. The reflectivity is measured in a fashion similar to that described in the previous section. The transmissivity, however, is measured by analyzing the voltage waveform $g(k)$ for a node in the substrate such as node 160. If g_{max} represents the peak value for the last 100 iterations of the sinusoidal signal $g(k)$, then:

$$T = \left(\frac{g_{max}}{E_{max}}\right)^2,$$

$$A = 1 - T - R \tag{70}$$

where A is the absorptivity of the film. Figure 10 shows the reflectivity pattern for an absorbing thin film with $n_1 = 1$, $n_{re} = 2$, $n_3 = 1.5$, and $n_{im} = 0$, 0.1 and 0.2. The transmissivity of the film is shown in Fig. 11 for the same values on n_1, n_2^* and n_3. From the layout of the theory and algorithm of this model, it can be considered as a time domain method that can accommodate the physical problem after being "translated" into an appropriate electrical network of elements that correspond to the full features of the original problem. Once this is accomplished the burden is removed from the physicist to the machine which can be a personal computer

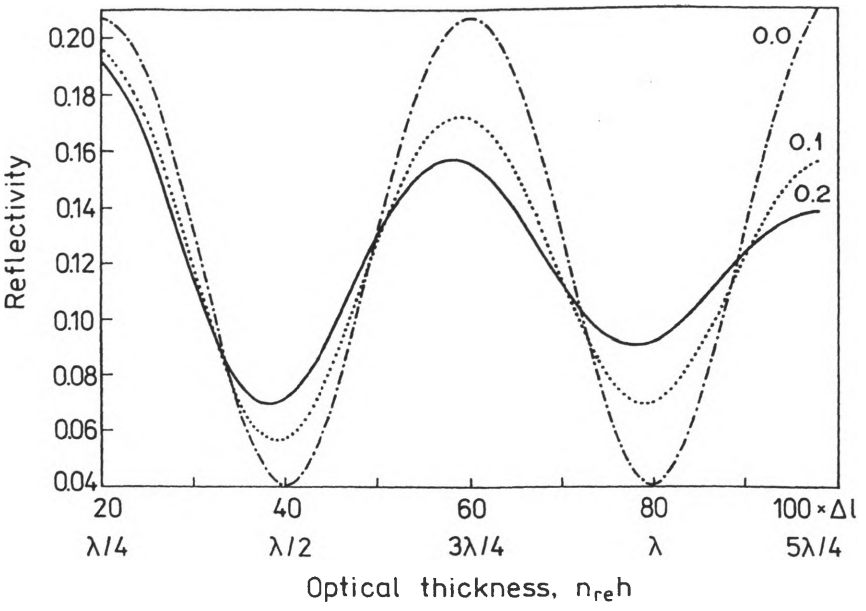

Fig. 10. Calculation of the reflectivity R versus the optical thickness $n_{re}h$ for two absorbing thin films whose indices of refraction are $n = 2.0+0.1j$, $2.0+0.2j$ displaced simultaneously with a thin dielectric film of $n = n_{re} = 2.0$

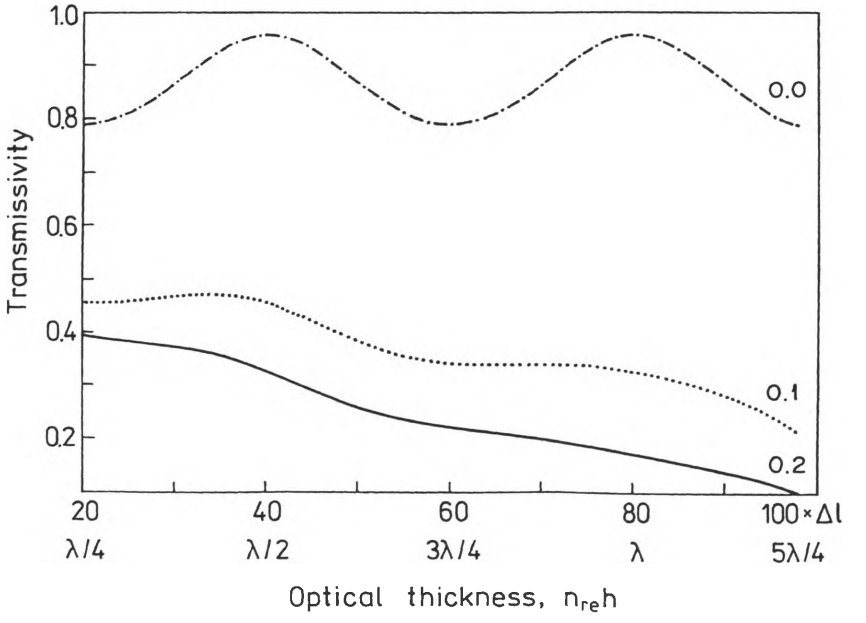

Fig. 11. Calculation of the transmissivity T versus the optical thickness $n_{re}h$ for two absorbing thin films whose indices of refraction are the same as in Fig. 10

that is available almost to every worker in the field. The simplicity of the TLM algorithm enables easy implementation on a personal computer using any high level language (Turbo Pascal in this case). The characteristic method technique adopted earlier by the author, on the other hand, requires manipulation of matrices whose elements are complex numbers, which restricts the use of computer language to Fortran. Moreover and equally important is to mention that accuracy of the results is not at all hampered by this model. As a matter of fact, a greater accuracy can always be obtained by using a finer mesh. The only requirements from the PC are more memory and time, both of which are available in today's powerful personal computers.

In conclusion, an efficient computational method for calculating the optical properties of thin films regardless of thickness, material and range of wavelengths has been established. This method does not only compete with other methods such as the CMT but also allows possible replacement of such methods when dealing with multilayer systems and superlattices. This is due to the attractive advantage of avoiding the use of any complex quantities when dealing with absorbing layers as part of the constituents of a layer system, a cumbersome practice that is unavoiodable in the other methods. In addition to this, the interface between two different layers in multilayer structures can be accounted for by representing it by a corresponding stub in the picked equivalent network. The choice of the impedance of the stub corresponds to a certain composite of the material (n_{re} and n_{im} that stand for the index of refraction and extinction coefficients widely referred to as n and k, respectively). Thus a series of values for this impedance for a certain interface should provide the investigator with the possible optical properties of the system. Among these results, those nearest to the experimental ones can be chosen. This would then be a tool to assign the most accurate optical constants that could correspond to the empirical results. Achieving this by coupling the technique with an optimization routine that varies the physical and geometrical parameters of the optical system under study can also serve to arrive at the required design of the system at a stage before its fabrication. Another application of this method is the computation of the first and second order derivatives of the optical properties: reflectivity R, transmissivity $T$and absorptivity A for any multilayer system. This should provide the points of extrema for the spectral dependence of the optical properties of the layer system. From the physical parameters and the optical constants of such a layer system its main characteristic features can then be unravelled even before manufacturing it.

A final advantage of this method over previous methods is the ease with which oblique incidence and not only normal incidence of e.m. waves on a film can be treated. This can be accomplished by an adaptation of the two dimensional TLM model introduced successfully by JOHNS and BEURLE [6] for solving waveguide problems.

Acknowledgment – The author would like to express his appreciation to Samer A. J. Abu El-Haija from the Electrical Engineering, University of Colorado, USA, for his assistance and help with the computer program used in this problem.

References

[1] ABU EL-HAIJA A. J., MCMARR P. J., MADJID A. H., Appl. Opt. **18** (1979), 3123.
[2] MADJID A. H., ABU EL-HAIJA A. J., Appl. Opt. **19** (1980), 2612.
[3] ABELES F., Ann. Phys. (Paris) **5** (1950), 596.
[4] THELEN A. J., J. Opt. Soc. Am. **56** (1966), 1533.
[5] BORN M., WOLF E., *Principles of Optics*, 6th ed., Pergamon Press, New York 1980.
[6] JOHNS P. B., BEURLE R. L., Proc. IEE **118** (1971), 1203.
[7] JOHN P. B., IEEE Trans. Microwave Theory Tech. **22** (1974), 209.
[8] HOEFFER W. J. R., IEEE Trans. Microwave Theory Tech. **33** (1985), 882.
[9] PULKO S., MALIK A., JOHNS P. B., Int. J. Numer. Methods Eng. **23** (1986), 2302.
[10] AL-ZEBEN M. Y., SALEH A. H. M., AL-OMAR M. A., Int. J. Numer. Modelling; Elect. Networks, Devices and Fields **5** (1992), 219.
[11] SALEH A. H. M., Int. J. Numer. Modelling, Elect. Network, Devices and Fields **2** (1989), 53.
[12] ABU EL-HAIJA A. J., MADJID A. H., Phys. Status Solidi B **140** (1987), 113.
[13] HEAVENS O. S., *Optical Properties of Thin Solid Films*, Butterworth Sci. Publ., London 1955.

Received February 18, 1997